882 *Biochemistry* **2010,** *49,* 882–892
DOI: 10.1021/bi901478f

BIOCHEMISTRY
including biophysical chemistry & molecular biology
Article

Band Shape Heterogeneity of the Low-Energy Chlorophylls of CP29: Absence of Mixed Binding Sites and Excitonic Interactions†

Erica Belgio, Anna Paola Casazza,‡ Giuseppe Zucchelli, Flavio M. Garlaschi, and Robert C. Jennings*

Istituto di Biofisica del CNR, sede di Milano, e Dipartimento di Biologia, Università degli Studi di Milano, via G. Celoria 26, 20133 Milano, Italy. ‡*Present address: Istituto di Biologia e Biotecnologia Agraria (IBBA) del CNR, via Bassini 15, 20133 Milano, Italy*

Received August 24, 2009; Revised Manuscript Received January 4, 2010

ABSTRACT: A number of spectroscopic characteristics of three almost isoenergetic, red-shifted chlorophylls (chls) in the PS II antenna complex CP29 are investigated with the aim of (i) determining whether their band shapes are substantially identical or not, (ii) addressing the topical problem of whether they are involved in excitonic interactions with other chls, and (iii) establishing whether their binding sites may be defined as "mixed" with respect to their capacity to bind chls *a* and *b*. The three chls A2-CHL612, A3-CHL613, and B3-CHL614 were analyzed after *in vitro* apoprotein−pigment reconstitution using the CP29 coding sequence from *Arabidopsis thaliana* for both the wild-type and mutant complexes. Difference spectra thermal broadening analyses indicated that the half-bandwidths varied between 12 and 15 nm (at room temperature), due mainly to differences in the optical reorganization energy (25−40 cm^{-1}). Moreover, only the A2 chl displayed an intense vibrational band in the 300−600 cm^{-1} interval from the 0−0 transition. We conclude that within the red absorbing (∼680 nm) antenna chls of a single chl−protein complex a marked spectral band shape heterogeneity exists. By analysis of the absorption and circular dichroism spectra no evidence was found of significantly strong excitonic interactions. The single gene mutation of the A3 and B3 binding sites causes absorption changes in both the long wavelength chl *a* absorbing region and in the chl *b* spectral region. This has previously been observed and was attributed to "mixed" chl *a*/*b* binding sites [Bassi, R., Croce, R., Cugini, D., and Sandona, D. (1999) *Proc. Natl. Acad. Sci. U.S.A. 96*,10056−10061]. This interpretation, while in principle not being unreasonable, is shown to be incorrect for these two chls.

It is well-known that in the antenna complexes of plant PS[1] II the energy spread of the Q_y absorption band is about 30 nm ($3k_BT$ at room temperature, where k_B is the Boltzmann constant and T is the absolute temperature) while that of the core antenna is slightly narrower, 25 nm ($2.5k_BT$ at room temperature) (e.g., ref *1*). This quite large energy disorder distribution leads, at excited state equilibration, to a high excited state population probability in the lower energy chl forms which, in the case of the outer antenna complexes and at room temperature, is approximately 20 times greater that in the highest energy chls. In addition, linear dichroism measurements suggest that the low-energy forms of all chl−protein complexes are preferentially located in the membrane plane (*2*) while the higher energy forms are not. This would lead to the low-energy forms, bound to different complexes, having dipole−dipole orientations favoring rapid energy transfer. These simple observations suggest the possibility that these low-energy chl *a* forms may be preferentially involved in intercomplex transfer and may thus be peripherally located in these complexes. While much picosecond and subpicosecond data on exciton dynamics in isolated complexes (*3*) have been obtained in recent decades, still little is known about intercomplex transfer. This latter process, due to greater interchromophore nearest-neighbor distances between complexes (*4*), will presumably lead to slower energy transfer between complexes than within the complexes themselves. Intracomplex energy transfer is known to be extremely rapid with equilibration being substantially complete in a few picoseconds (*5*). However, despite this extremely rapid transfer within antenna complexes, it has become increasingly obvious, in recent years, that kinetically limiting energy transfer processes do, in fact, occur in the antenna (*6*, *7*), leading to a substantial diffusion-limited component to photochemical trapping. This limitation has been suggested to be mainly located at the internal antenna−reaction center interface (*8*) though recent data of Miloslavina et al. (*9*) and Tumino et al. (*10*) contest this. We are therefore of the opinion that the kinetically limiting energy transfer processes are based well inside the antenna and probably at the antenna complex interfaces. For this reason it would not be surprising that the low-energy forms, which have a high excited state population probability, are located at the complex interfaces in order to render intercomplex transfer as fast as possible. Thus these chls are particularly worthy of detailed study. We emphasize that the energy transfer rate scales linearly with the excited state probability of the donor pigment in the Förster transfer model approach (*11*).

Biochemical data, and more recently crystallographic data (*12*−*14*), indicate that the three minor external antenna complexes (CP24, CP26, and CP29), while not having a very significant light harvesting role (*15*), seem to be physically placed between the major external antenna complex (LHCII) and the

†Financial assistance was partially provided by PRIN 2007.
*Corresponding author: e-mail, robert.jennings@unimi.it; tel, +39025-0314858; fax, +390250314815.
[1]Abbreviations: chl, chlorophyll; CD, circular dichroism; CP, chlorophyll−protein complex; fwhm, full width at half-maximum; OD, optical density, OS, overlapping structure; PS, photosystem; wt, wild type.

 Published on Web 01/04/2010

core antenna and hence have a bridge-type role in transferring energy into the core antenna (CP43 and CP47). In order to initiate a series of investigations on the possible role of the low-energy chls in intercomplex transfer, we have started out by examining a number of the physicochemical properties of the three lowest energy chls in CP29. Three main points are addressed. We ask the questions as to (i) whether the three, almost isoenergetic low-energy chls of CP29, chls A2-CHL612, A3-CHL613, and B3-CHL614, have similar physical properties, and hence similar band shapes, or whether there are significant differences between them at the level of bandwidths, electron/phonon coupling, and vibrational band structure (this question of heterogeneity of antenna chlorophyll properties within a single chlorophyll−protein complex has not previously been addressed); (ii) whether these chls are essentially monomeric or, alternatively, are involved in excitonic type interactions with other chls, with a possible redistribution of their dipole strengths; (iii) whether the A3-CHL613 and B3-CHL614 chl binding sites may be considered "mixed" chl *a*/*b* binding sites.

Direct evidence for chl band shapes for protein-bound chls, at physiological temperatures, has proved difficult to obtain. Zucchelli et al. (*16*) calculated room temperature band shapes based on the hole burning data collected at a temperature close to 2 K (*17*). Bassi et al. (*18*) and Zucchelli et al. (*19*), using site-directed mutational techniques, obtained and analyzed spectroscopically, at room temperature, the A2-CHL612 chl difference spectrum (wt *minus* mutant) of the CP29 reconstituted complex. This chl seems to possess some peculiarities with respect to solvated chl and, in particular, displays a marked room temperature absorption structure which overlaps with the main Q_y band. The source of this structure has not been defined to date and is analyzed here. Line-narrowing spectroscopies (*20*), which have provided important information on electron/phonon coupling and thus, in principle, also on absorption band shapes at 2−4 K, suffer from the problem that the particular chl site investigated is often impossible to define, and the necessity to use very low temperatures renders conclusions concerning physiologically more relevant temperatures difficult.

The approach used in the present paper has the advantage of permitting the study of specifically identified chls, and there are no temperature restrictions on measurements. It is based on the reconstitution of the CP29 apoprotein, overexpressed in *Escherichia coli*, with the appropriate pigments. This technique for CP29 was pioneered by Bassi and co-workers (*18*). Absorption, fluorescence, and CD spectroscopies of the recombinant wt and mutant complexes were performed and the difference spectra calculated.

While this study was in an advanced state a paper by Mozzo et al. (*21*) was published which provided information on one of the low-energy chls of CP29 which we have also examined (A2-CHL612). As there are differences between their conclusions and ours, on some aspects, we have dedicated special attention to this chl. The chl nomenclatures used are due to Kühlbrandt (*22*) and Liu et al. (*23*) for LHCII and used for CP29 on the basis of its high sequence homology with LHCII (*18*).

MATERIALS AND METHODS

Recombinant CP29 Complexes. The *Lhcb4.1* coding sequence corresponding to the mature form of CP29 was amplified via RT-PCR (Promega) from total RNA extracted from *Arabidopsis thaliana* (TRIZOL reagent; Invitrogen), using primers (MWG-Biotech) carrying the restriction sites for *Nco*I and *Eco*RI (New England Biolabs). The digested PCR product was cloned (ligation kit; Promega) into the pET32b expression vector (Qiagen) after the excision of the Trx coding sequence. The construct was checked by DNA sequencing (BMR Genomics s.r.l.). For the A2-CHL612 mutation the histidine 216 was substituted by a phenylalanine via site-directed mutagenesis (mutagenesis kit; Stratagene) on the 6×His-CP29pET32b plasmid. For the A3-CHL613 the substitution was glutamine 230 with leucine, and for the B3-CHL614 histidine 245 was replaced with leucine.

The N-terminal His-tagged CP29s (wild type, CP29wt, and mutated CP29a2, CP29a3, CP29b3) were expressed in the BL21 *E. coli* strain (Invitrogen) in the form of inclusion bodies which were purified following ref *24*.

Reconstitution was performed as described by Giuffra et al. (*25*), incubating inclusion bodies with pigments using the recommended chl *a*/*b* ratio of 8, which yields a CP29wt reconstituted complex with a chl *a*/*b* ratio of 3.0 ± 0.2 (five reconstitutions), in agreement with the known chl binding stoichiometry of six chl *a* and two chl *b* (*26*). The standard deviation is due to the different reconstitutions as the measurement errors for any one preparation are diminishingly small. This is close to the chl *a*/*b* ratio reported for the native CP29 extracted from plants (e.g., ref *27*) and is also the same as previously reported values for the reconstituted complex (e.g., ref *28*).

For the CP29a2 mutant we measured a chl *a*/*b* ratio of 2.5 ± 0.2 (seven reconstitutions), consistent with the removal of one chl *a*, while that for the A3-CHL613 mutant was 2.7 ± 0.2 (three reconstitutions), which probably also indicates removal of one chl *a*. The chl *a*/*b* ratio of the B3-CHL614 mutant was 3.5 ± 0.1 (five reconstitutions). An increased chl *a*/*b* ratio for this latter mutant was previously reported (*18*). This high chl *a*/*b* ratio will be further mentioned in the Discussion.

Total pigments were extracted from spinach and barley (*chlorinaf2* mutant) thylakoids with 80% acetone (*29*). Xanthophylls were purchased from Sigma. Pigment concentration was calculated from absorption measurements according to refs *30* and *31* and checked by HPLC.

Recombinant reconstituted complexes were purified by affinity chromatography using a Ni^{2+}-NTA resin (Qiagen).

Spectroscopy. Absorption and fluorescence spectra of recombinant complexes were measured between 80 and 285 K with a liquid nitrogen cooled CCD array detector (Princeton Applied Research) through a spectrograph (Spectra Pro-300i; Acton Research Co.) equipped with a 300 grooves/mm grating. The wavelength scale of the instrument was calibrated with a neon spacing calibration source (Cathodeon). The spectral resolution of this setup is 0.28 nm. The excitation beam (440 nm) was provided by a water-cooled xenon lamp and monochromator of a J-500 spectropolarimeter (Jasco). Fluorescence spectra were corrected for the instrument detection wavelength sensitivity. Samples were diluted to 0.4 OD/cm at the Q_y absorption maximum for absorption measurements and to 0.1 OD/cm for fluorescence, in a buffer containing 10 mM Hepes, pH 7.6, 0.045% DM, and 60% glycerol (v/v).

Low-temperature absorption measurements down to 80 K have been performed using a cryostat (Oxford Optistat CF) with a 1 cm path length cuvette. The temperature was measured by a sensor directly in contact with the sample and monitored by a controller (Oxford ITC 503) that regulates also the temperature changes.

The CD spectra were measured at 10 °C in a Jasco 600 spectropolarimeter equipped with a red extended photomultiplier

tube (Hamamatsu R2228). The wavelength step resolution was 1 nm with a maximum scan rate of 10 nm/min and a bandwidth of 2 nm. Four independent recombinant preparations were analyzed. The spectra were normalized to the pigment content on the basis of the area subtended by the absorption spectra in the 620−720 nm region and using a ratio of 0.7 between the extinction coefficients of chl *b* and chl *a*.

Thermal Broadening Analysis. In order to determine both the optical reorganization energy ($S\nu_m$), of the Q_y absorption band of the A2-CHL612, A3-CHL613, and B3-CHL-614 chls, which yields information on excited state pigment coupling (S) to protein phonons of mean frequency ν_m, as well as the site inhomogeneous broadening, we have used a previously described approach (*32*) and have analyzed the thermal broadening of the absorption bands in terms of a model in which excited state electrons are quite strongly coupled to a single mean phonon frequency. This model is derived from the extensive hole burning studies of chl−protein complexes of Small and collaborators (*33*). In this hypothesis, the full width at half-maximum of the homogeneously broadened pigment absorption ($fwhm_{hom}$, cm^{-1}) is given by

$$fwhm^2_{hom} = (8 \ln 2) S\nu_m^2 \coth(h\nu_m c/2k_B T) \quad (1)$$

where S is the Huang−Rhys coupling strength, ν_m (cm^{-1}) is the mean phonon frequency associated with protein vibrations, c is the velocity of light, h is the Planck constant, k_B is the Boltzmann constant, and T is the absolute temperature. For chl−protein complexes ν_m has been determined to have a value close to 20 cm^{-1}. Thus, for temperatures greater than 70 K, $h\nu_m c \ll 2k_B T$ and $\coth(x) \sim x^{-1}$ so that eq 1 may be well approximated by

$$fwhm^2_{hom} = (16 \ln 2)(k_B/hc) S\nu_m T \approx 7.7 S\nu_m T \quad (2)$$

In addition to homogeneous broadening, pigment spectra in chl−protein complexes are also subject to the inhomogeneous broadening ($fwhm_{inh}$) associated with statistical fluctuations in the binding sites, which lead to a statistical distribution of absorption energies. Inhomogeneous broadening is generally assumed to be independent of temperature and is frozen in at low temperatures. Thus, the overall fwhm for Gaussian absorption bands is given by

$$fwhm^2 = 7.7 S\nu_m T + fwhm^2_{inh} \quad (3)$$

Therefore, the analysis of the fwhm as a function of temperature in the range 80−300 K permits determination of the optical reorganization energy ($S\nu_m$) and the $fwhm_{inh}$ of the pigment absorption band.

RESULTS

As we are interested in the redmost absorption bands of CP29, we initially consulted the earlier mutational and absorption study of Bassi et al. (*18*). According to this analysis the A2-CHL612 difference spectrum peaks near 680 nm and the B3-CHL614 near 679 nm, and so site-directed mutations focused at eliminating these chls were performed. We also noticed that the A3-CHL613 difference absorption spectrum had its absorption peak in this same wavelength interval, and so this chl was also taken into consideration. That these three chls are all in the low-energy absorption wing of reconstituted CP29wt is readily seen in Figure 1 where the steady-state fluorescence emission spectra for the wt and mutant complexes are presented. We present here the fluorescence spectra, and not the absorption spectra, as these

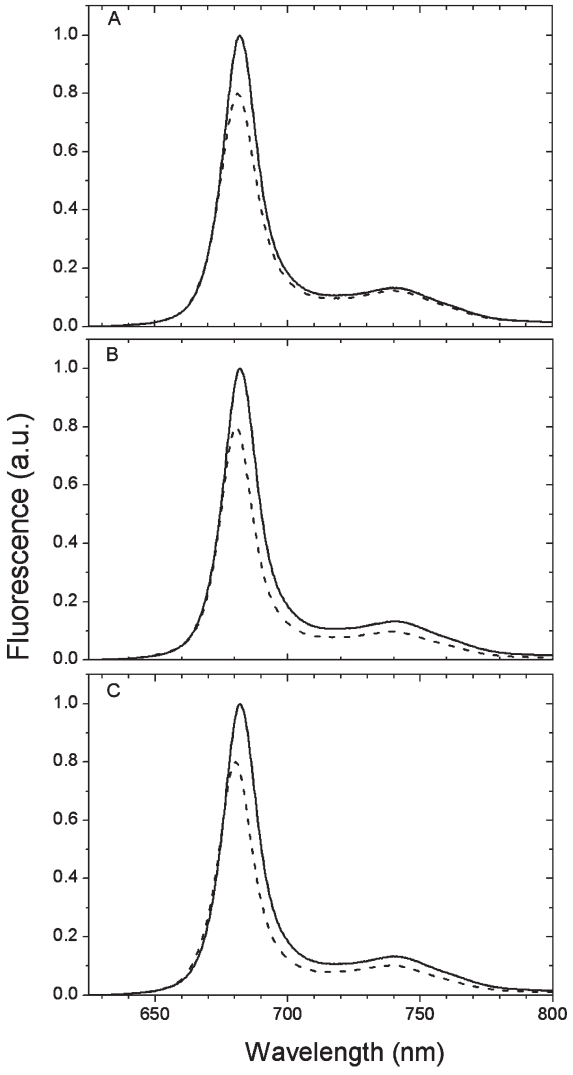

FIGURE 1: Room temperature fluorescence spectra of CP29 wild-type (continuous line) and mutant (dashed line) complexes normalized on the assumption of the mutational induced loss of one chl *a* (see text and Figures 4−6): (A) CP29a2; (B) CP29a3; (C) CP29b3.

underline the low-energy nature of all three missing chls in the mutated complexes, due to their high excited state population in the wt complex.

In Figure 2 the wt CP29 absorption, measured at 77 K, is overlaid with that of the native complex, extracted from maize. Our reconstituted complex, while displaying a small blue shift with respect to the native one, has a similar overall structure. This blue shift is also evident in reconstituted CP29 produced by the Bassi group and measured in our laboratory (*28*) (data not shown), which indicates that this is a characteristic of reconstituted CP29 complexes thus far produced. The small secondary peaks near 640 and 652.5 nm are the two chl *b* molecules.

In the past we have used the Stepanov relation (*34*)

$$F(\nu)/A(\nu) \propto C(T)\nu^3 e^{-(h\nu/k_B T)} \quad (4)$$

between absorption $A(\nu)$ and fluorescence $F(\nu)$ spectra to decide whether the complexes are in a completely equilibrated state in which uncoupled pigments are absent. C is a temperature-sensitive constant, h is the Planck constant, and k_B is the Boltzmann constant. In Figure 3 it is shown that also in this case the measured and calculated fluorescence spectra of reconstituted CP29wt and the three mutant complexes are in good

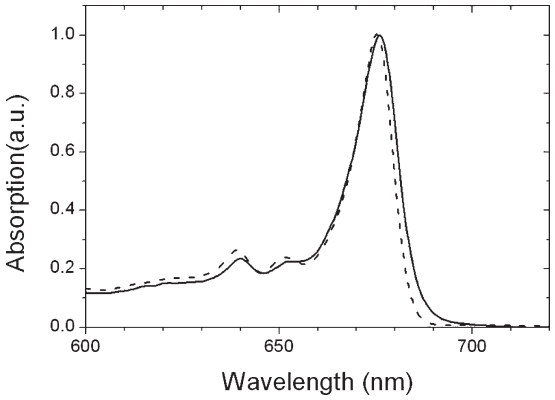

FIGURE 2: 77 K absorption spectra of native (continuous) and wild-type reconstituted (dashed) CP29 complexes. The spectra were normalized at their maxima.

agreement in the region of absorption/fluorescence spectral overlap. Data are presented for the 285 K spectra. However, a close match is also found down to about 180 K (data not presented). We therefore conclude that the complexes are thermalized and uncoupled pigments are absent. These data also indicate that the preparations are rather homogeneous, as heterogeneous complex absorption spectra and possibly different fluorescence yields lead to deviations from correct Stepanov behavior (*35*).

We therefore performed pigment reconstitution experiments with these three mutated proteins and the wt. The mutant and wt complex absorption spectra are presented at different temperatures in Figures 4−6 together with the relevant wt *minus* mutant difference spectra. In the following we will discuss the characteristics of these spectra.

A2-CHL612 Chl Site Mutation. In order to compare the wt and mutant spectra, it is necessary to use a spectral normalization procedure. This was achieved on the basis of the known chl *a*/*b* ratio of 3 for both the native and the wt reconstituted complexes (see Materials and Methods section), which is generally interpreted in terms of the binding of six chl *a* and two chl *b* molecules per complex (e.g., ref *28*). On this basis, and using the measured *a*/*b* ratio of 2.5 for the CP29a2, together with the known relative dipole strengths of the two chl types, taken as $b/a = 0.7$, the CP29a2 absorption spectrum was appropriately normalized (see Figure 4 and its legend) and the 285K difference spectrum determined (Figure 4D). This difference spectrum is in close agreement with the published one (*18*), peaking near 680 nm, with a Q_y fwhm of about 12 nm and a prominent overlapping structure (OS) on the short wavelength side. Upon lowering the temperature, the expected Q_y band narrowing occurs, and the difference absorption spectrum shifts slightly toward higher energies (Figure 4C). At 80 K the maximum is at about 676 nm, and the OS is clearly resolved from the main Q_y transition band. The absence of absorption changes at other wavelengths suggests that the A2-CHL612 chl is essentially a monomer, as, due to dipole strength redistribution, interaction with other chls would lead to absorption structures in the difference spectrum also at wavelengths other than 680 nm. This interpretation is correct if it can be demonstrated that the OS is, in fact, a vibrational band.

In order to establish whether the OS is due to vibronic coupling to the main Qy electronic transition, we have searched for its fluorescence mirror image in the emission difference spectra. Two such examples, at 285 and 80 K, are presented in Figure 7. At 285 K the mirror image structure is just discernible in the fluorescence

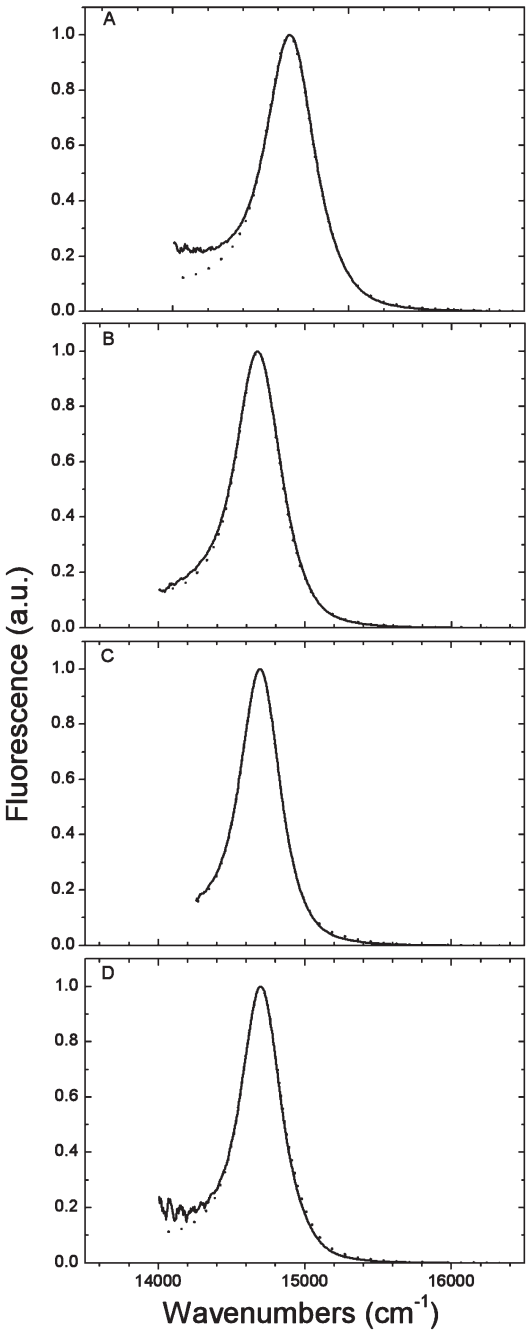

FIGURE 3: Comparison between calculated (dotted line; eq 4) and measured (solid line) steady-state fluorescence spectra of reconstituted CP29 complexes. (A) CP29wt; (B) CP29a2; (C) CP29a3; (D) CP29b3.

difference spectrum and can be detected in the second derivative spectrum (data not presented). It is clearly present in the 80 K spectrum. The numbers on the Figure (300−600 cm^{-1}) indicate the wavenumber separation with respect to the absorption/fluorescence mirror symmetry axis.

We have also investigated whether the A2-CHL612 chl may interact excitonically with other chls by means of circular dichroism measurements in the Q_y absorption region. Excitonic interactions involving the A2-CHL612 chl are expected to modify the CD spectrum of the mutant also at wavelengths other than near 680 nm. Owing to the recent suggestion of a small positive CD structure near 665 nm, which was interpreted in terms of an excitonic interaction with the A2 chlorophyll (*21*), we analyzed

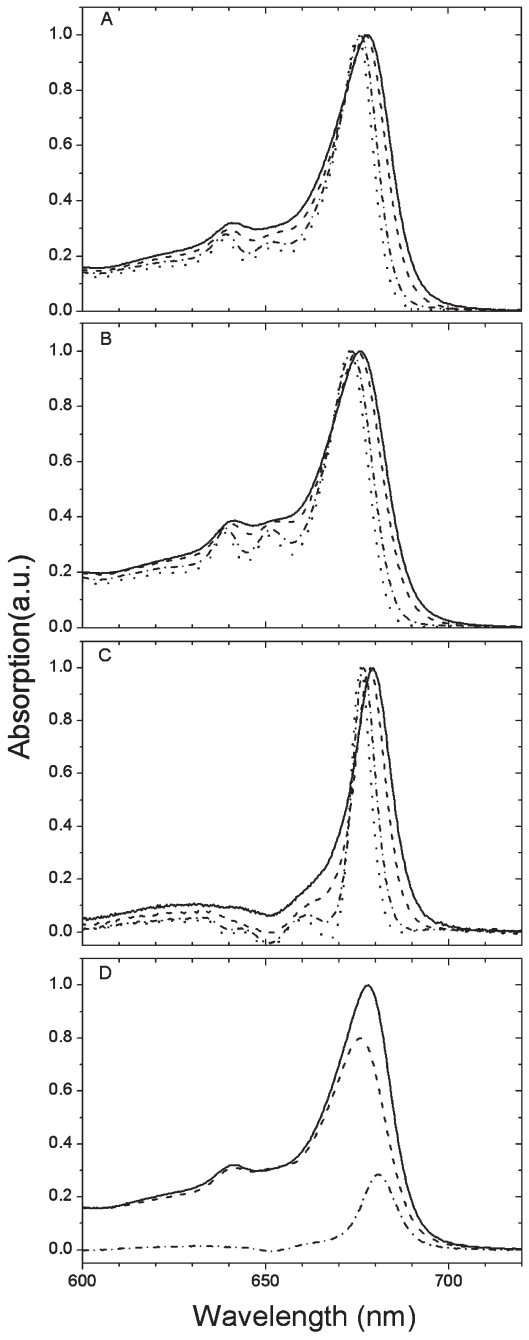

FIGURE 4: Absorption spectra of reconstituted CP29 complexes measured at different temperatures (285 K, solid line; 245 K, dashed line; 160 K, dashed-dotted line; and 80 K, dotted line). (A) CP29wt; (B) CP29a2; (C) difference CP29wt *minus* CP29a2 at each temperature. The spectra are normalized at their maxima. (D) Room temperature absorption spectra of wt (solid line) compared to the appropriately normalized mutated complex (dashed line) and the difference spectrum (dashed-dotted line). For the normalization procedure, see Results. In this case the normalization factor was 0.86.

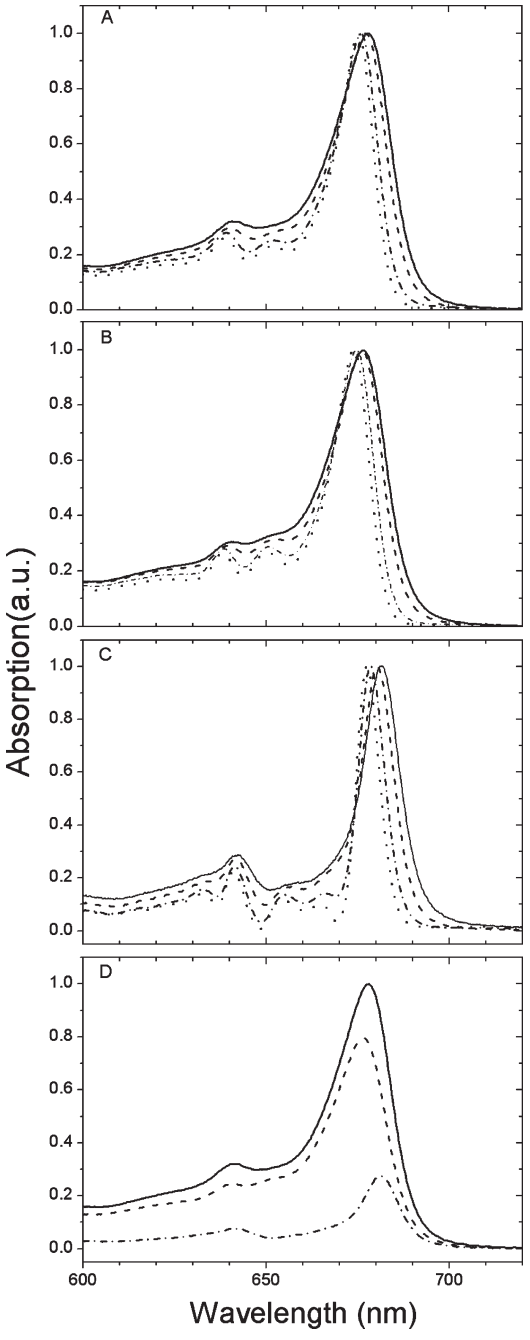

FIGURE 5: As in Figure 4 but for the CP29a3 complex. The normalization factor was 0.84.

this in detail. Over 20 separate CD measurements, using many different CP29a2 and wt reconstituted complexes, were performed in order to determine the measurement errors. These are indicated on the spectra (Figure 8A). It should first be noted that these spectra are clearly nonconservative in the wavelength interval of our measurements, and it is well-known that this is also the case when the entire visible spectral interval is considered (e.g., ref *25*). This nonconservative CD spectrum is also characteristic of most chl−protein complexes. To the best of our knowledge no clear explanation for this is available. The wt spectrum has a dominant (negative) lobe, which peaks close to 681 nm and which is therefore red shifted by approximately 4 nm with respect to the absorption maximum of the complex, with a small positive lobe near 665 nm. Both of these structures are associated with chl *a*. The bimodal negative lobe at 640 nm and near 650 nm is associated with the two chl *b* molecules which absorb at these wavelengths (Figure 4A). This spectrum of the reconstituted wt complex is almost identical to that published by Pascal at al. (*36*) for the native CP29.

We now consider the CD spectrum of the CP29a2 mutant (Figure 8A). The results, for the Q_y spectral region, show a large decrease in the negative lobe which accounts for about 30% of the total intensity of this lobe when evaluated after normalization to the corresponding absorption. It is interesting to note that the

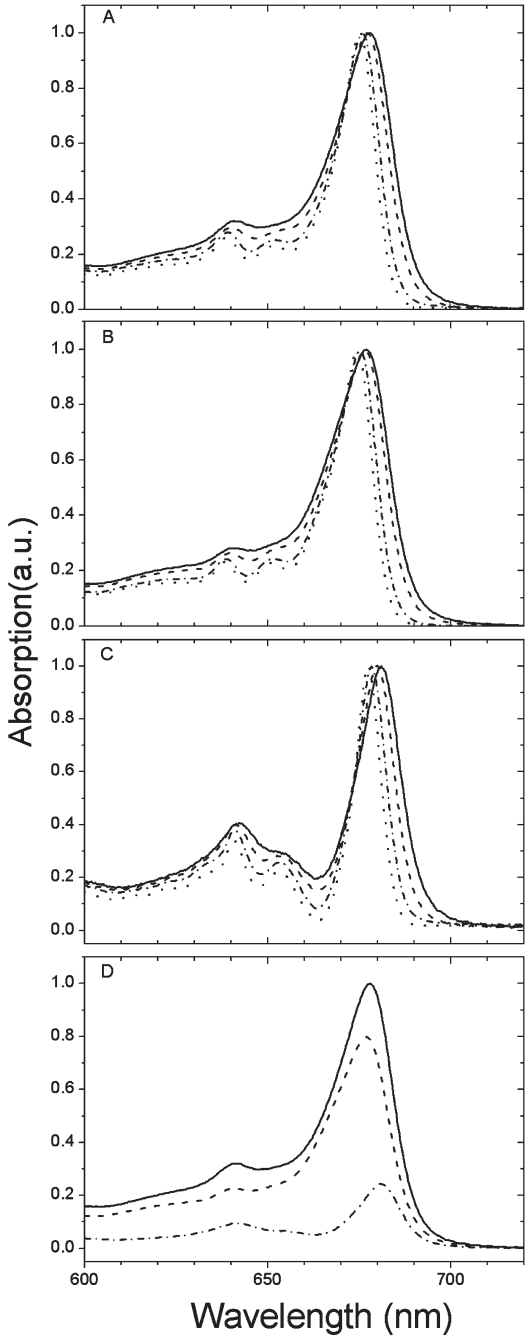

FIGURE 6: As in Figure 4 but for the CP29b3 complex. The normalization factor was 0.82.

band shape of the negative lobe remains almost unchanged in the CP29a2 mutant with respect to the wt complex (unpublished data) and no other significant spectral changes are apparent within the estimated error distribution. As mentioned above, the decrease in the negative lobe of the mutant complex is large, much larger than the CD signal usually associated with a chl monomer (*37*). However, intense optical activity may be induced in monomers due to structural deformation of the molecule, in this case induced by the protein. There are several suggestions in the literature for an intense "intrinsic" CD signal at specific chl binding sites in the D1/D2/cyt *b*-559 complex (*38*) and for a red-shifted antenna chlorophyll, absorbing at 679 nm, in the alga *Pleurochloris meiringensis* (*39*, *40*). In the present context it may be significant that, in LHCII, it is in fact the A2-CHL612 which has been suggested to display the greatest waving deformation of

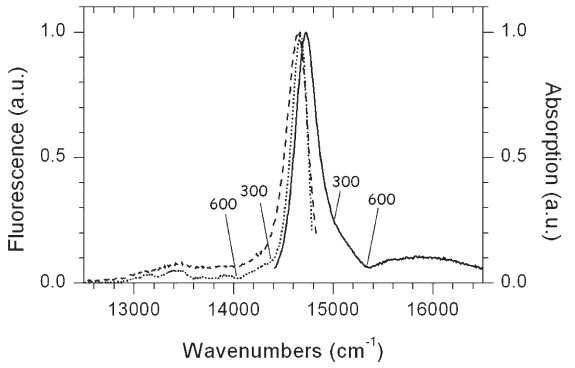

FIGURE 7: Mirror symmetry representation of the 285 K steady-state absorption (solid line) and fluorescence (dashed line) spectra of the A2-CHL612 chl, obtained as the difference spectra (CP29wt *minus* CP29a2). The 80 K emission difference spectrum is also presented (dotted line). The numbers on the figure delimit the wavenumber interval, with respect to the symmetry axis, in which the OS structure is visible.

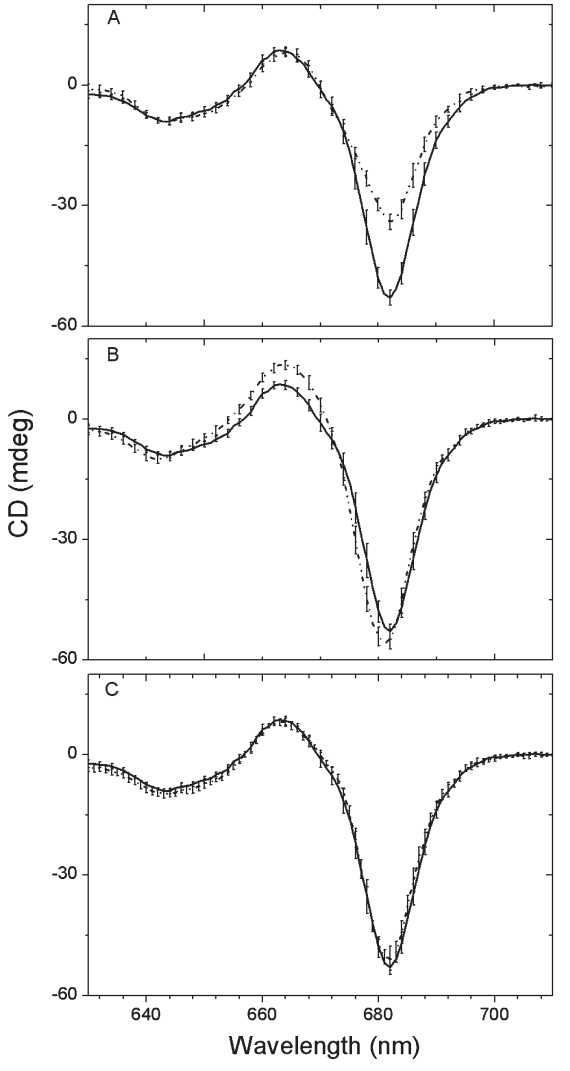

FIGURE 8: CD spectra of CP29wt (solid line) and mutant complexes (dashed lines) normalized to the absorption. (A) CP29a2; (B) CP29a3; (C) CP29b3. The error bars are the measurement standard deviations.

the porphyrin ring structure, with respect to the chlorin plane (*41*). We note also that the presence of intense monomer

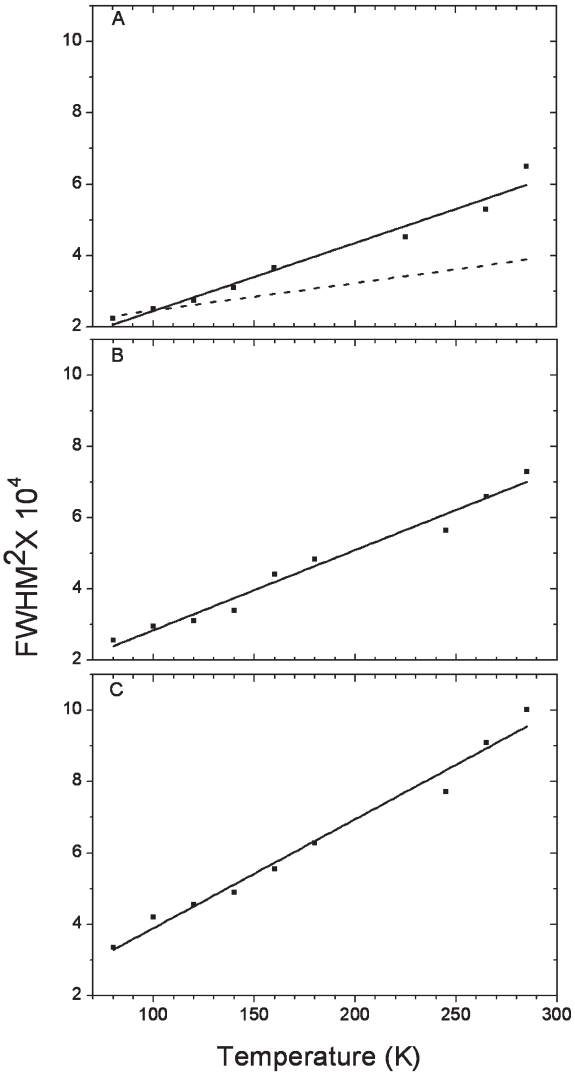

FIGURE 9: Square of the fwhm as a function of temperature for the Q_y absorption band of (A) chl A2-CHL612, (B) chl A3-CHL613, and (C) chl B3-CHL614. In each case, the solid straight line is the linear regression fit (r = 0.95−0.97) of an average fwhm over three CP29 recombinant preparations. The dashed line was obtained using the $S\nu_m$ and $fwhm_{inh}$ values published by Pieper et al. (see text).

CD signals provide a possible and simple explanation for the markedly nonconservative nature of the CD spectra of isolated complexes.

The optical reorganization energy ($S\nu_m$) and the $fwhm_{inh}$ of the Q_y absorption band of the A2-CHL612 pigment were determined as described in the Materials and Methods section (Figure 9A) and yield an $S\nu_m \approx 25\ cm^{-1}$ with a $fwhm_{inh} \approx 70\ cm^{-1}$. The value of $S\nu_m$ is within the range usually reported for antenna chls using line narrowing techniques (*42*) at 2−4 K, while the inhomogeneous contribution is somewhat lower, with reported values between 100 and 150 cm^{-1} being more common (*43*).

A3-CHL613 Chl Site Mutation. As already described for the CP29a2 mutant the wt *minus* chl A3-CHL613 mutant difference spectra were determined between 80 and 300 K (Figure 5C). The room temperature difference spectrum displays a main band peaking near 681 nm, and in addition, the 640 nm chl *b* absorption is also clearly evident, with a small structure near 655 nm (Figure 5D). The area subtended by the chl *a* Q_y band constitutes 80% of the total difference spectrum area which we interpret as indicating that the A3-CHL613 site is essentially a chl *a* binding site. The presence of the chl *b* signals in the difference spectrum is discussed in detail in the Discussion.

The main chl *a* Q_y band, as for the A2-CHL612 chl, has a fwhm of about 12 nm at room temperature. The vibrational OS, present in the A2-CHL612 chl in both absorption and fluorescence, seems to be absent in the case of the A3-CHL613 chl. This has been confirmed by measurement of the fluorescence spectra down to 80 K (data not shown). Upon lowering the temperature, the expected Q_y absorption band narrowing occurs, and it shifts slightly toward higher energies (Figure 5C), in general agreement with measurements of the A2-CHL612 chl. At 80 K the maximum is at about 677.5 nm. In addition, the 655 nm structure observed at room temperature is sharpened, and another small band becomes evident near 665 nm. The CD spectrum, measured at room temperature, is presented in Figure 8B together with that of the wt. Small changes are apparent in the CP29a3 mutant with respect to the wt. The dominant negative lobe seems to have undergone a slight blue shift, which is of the order of 1 nm, and despite the rather large errors in the 680 nm region, a slight increase in the negative CD signal is apparent which is statistically significant. This is presumably associated with the chl A3-CHL613 absorption which peaks near 681 nm (Figure 5C). A clear and significant increase is also present in the positive lobe near 664 nm, which covers the wavelength interval from about 653 to 672 nm. This is the same wavelength interval in which small absorption decreases are detected (Figure 5C). No significant changes are evident in the 640−650 nm region associated with chl *b*. The possibility may be considered that these small increases in the CP29a3 mutant, and which are of opposite sign, may indicate the loss of a dimer-type signal, of weak intensity. Such a signal would carry a positive sign in the long wavelength region (around 680 nm) and a negative sign in the short wavelength region (665 nm). Thus the presence of an exciton involving the A3 chl cannot be excluded.

The optical reorganization energy of the Q_y band of the A3-CHL613 chl has been determined by means of the same thermal broadening experimental strategy as already described for the A2-CHL612 chl. The data are presented in Figure 9B. The homogeneous broadening (approximately 27 cm^{-1}) is similar to that for the A2-CHL612 chl and in the upper range of values usually reported for antenna chls from hole burning (*42*). The site inhomogeneous bandwidth is approximately 80 cm^{-1} which, as in the case of the A2-CHL612 chl (see above), is somewhat less than values indicated by hole burning.

B3-CHL614 Chl Site Mutation. As already described for the CP29a2 and CP29a3 mutants, the wt *minus* chl B3-CHL614 mutant absorption difference spectra were determined between 80 and 300 K. The room temperature difference spectrum (Figure 6D) displays a main band peaking near 680 nm, and in addition the 640 and 653 nm chl *b* absorptions are clearly evident (Figure 6C). The main chl *a* Q_y band has a fwhm of between 14 and 15 nm at room temperature and is, thus, somewhat broader than the Q_y band of the A2-CHL612 and A3-CHL613 chls. The vibrational OS, present in the A2-CHL612 chl, seems to be absent in the case of the B3-CHL614 chl, both in the room temperature and 80 K spectra. The area subtended by the chl *a* Q_y band constitutes 80% of the total difference spectrum area, which we interpret as indicating that the B3-CHL614 site is essentially a chl *a* binding site. The presence of the chl *b* signals in the difference spectrum is discussed in detail in the Discussion.

Upon lowering the temperature, the expected Q_y absorption band narrowing occurs and shifts slightly toward higher energies

(Figure 6C), in general agreement with measurements of the A2-CHL612 and A3-CHL613 chls. At 80 K the maximum is at about 676.5 nm.

The CD spectrum of CP29b3 (Figure 8C) cannot be distinguished from the spectrum of the wt complex, within experimental error. This would seem to exclude the possibility that this chl is involved in excitonic interactions with other pigments. This is particularly interesting as the absorption difference spectrum shows significant changes not only in the chl *a* region at 680 nm but also in the two chl *b* bands at 640 and 653 nm. This point will be dealt with in the Discussion section.

The optical reorganization energy of the Q_y band of the B3-CHL614 chl has been determined by means of the same thermal broadening experimental strategy as already described for the A2-CHL612 and A3-CHL613 chls. The data are presented in Figure 9C. The homogeneous broadening ($\sim$40 cm^{-1}) is greater than values obtained for the A2-CHL612 and A3-CHL613 chls and is approximately double the values for antenna chls usually reported from hole burning experiments (*42*). Thus either the Q_y transition is coupled more strongly to similar low-frequency phonon modes as the A2-CHL612 and A3-CHL613 chls or alternatively it is coupled to higher frequency modes. The inhomogeneous bandwidth is approximately 90 cm^{-1} which, as in the case of the A2-CHL612 and A3-CHL613 chls (see above), is somewhat less than values indicated by hole burning.

DISCUSSION

In the present study we have examined some of the physicochemical properties of three of the red-absorbing chl forms in the PS II antenna complex CP29 (chls A2-CHL612, A3-CHL613, and B3-CHL614). The main reason why these chls were chosen is that, by hypothesis, we consider that the low-energy chl forms, in which the excited state occupation probability is high with respect to the higher energy chls, may be directly involved in energy transfer between chl protein complexes (see the introduction). In the specific case of CP29, due to its location in the PSII antenna between the external antenna and the core (for recent review, see ref *44*), it has a particularly important function in intercomplex energy transfer between these two major antenna compartments. For the time being there is little experimental evidence on intercomplex energy transfer, and we are in the process of directly examining the involvement of the A2-CHL612, A3-CHL613, and B3-CHL614 chls. In this context it is necessary to understand the absorption and fluorescence band shape characteristics, necessary for determination of the Förster overlap integrals as it is the Förster mechanism that probably constitutes the energy transfer mechanism operative between chl−protein complexes. As excitonic calculations indicate that, in LHCII at least, one quite strong excitonic interaction exists between chls A2-CHL612 and B2-CHL611 (*23*, *45*), and recently Mozzo et al. (*21*) made a similar suggestion for CP29, in this paper we have asked the question as to whether the three red-absorbing chls of CP29 interact excitonically with other CP29 chls by the use of site-directed mutagenesis of chl ligands of the recombinant complexes together with circular dichroism measurements. In addition, we addressed the question as to whether these three almost isoenergetic CP29 antenna pigments have similar or dissimilar band shape structures due to changes in electron/phonon and vibronic coupling. To this end we have determined their optical reorganization energy and the inhomogeneous line widths.

In the recent theoretical study of Zucchelli et al. (*41*) it was shown, for the related complex LHCII, that porphyrin ring distortions of the different chl molecules displayed considerable heterogeneity which was shown to modify the chl absorption energies (spectral forms). These site-dependent distortions are also expected to modify the electron/phonon coupling and, thus, lead to band shape differences. In this paper we present clear experimental evidence that this is indeed the case for a group of isoenergetic chls. The room temperature bandwidths (fwhm) of the three red-absorbing chls (680−681 nm) vary between 12 nm for the A2-CHL612 and A3-CHL613 chls to 15 nm for the B3-CHL614 chl. These differences in the Q_y bandwidth are caused by the lower optical reorganization energy of the A2-CHL612 and A3-CHL613 pigments (25 and 27 cm^{-1}, respectively) and the somewhat higher value of 40 cm^{-1} for the B3-CHL614 chl. This latter value is in fact higher than those normally reported for PS II antenna chls using spectral line narrowing techniques, where values usually fall in the 15−27 nm range (e.g., ref *42*), similar to the A2-CHL612 and A3-CHL613 chls. Of interest in this respect is the paper by Pieper et al. (*46*) that analyzed what was considered to be the redmost chl of native CP29, the same complex as used in the present study. At their experimental temperature of 4 K this band absorbed near 678 nm, and the optical reorganization energy was determined to be about 10 cm^{-1}. This value is much lower than that determined for any of our three red-absorbing chls and yields a room temperature bandwidth of 8 nm rather than the values of between 12 and 15 nm which we found. In order to underline these large differences, we have overlaid the line representing their $S\nu_m$ and $fwhm_{inh}$ on our thermal broadening data for chl A2-CHL612 (Figure 9A, dashed line). As can be seen, the present results are not compatible with the absorption hole burning study when these data are used to calculate bandwidths at higher temperatures. These observations may indicate one of two possibilities. It may be that the 678 nm absorption transition, observed at 4 K in the hole burning studies, is not the same as any of the three chls investigated here (A2-CHL612, A3-CHL613, and B3-CHL614). This is a distinct possibility as none of these chls display an absorption maximum at 678 nm as reported by Pieper et al. (*46*). The second possibility is that the very low temperatures used in hole burning may modify the protein matrix and change the chl properties, influencing the characteristic optical microparameters. For example, the suggestion that a magnesium coordination change can occur at low temperatures has been made (*19*).

As can be seen from these studies, there is great spectral crowding and, inevitably, much electronic transition band overlap in the low-energy region of CP29. This may explain the differing values determined for the Huang−Rhys factor in the 680−688 nm range for fluorescence revealed holes (*47*). The broad inhomogeneous width ($\sim$130 cm^{-1}) reported in ref *46* could also be the result of the presence of holes burned in isoenergetic or near isoenergetic transitions. In the case of the present data the inhomogeneous width (75−90 cm^{-1}) is somewhat lower than the line narrowing data usually presented for measurements performed at 2−4 K (100−150 cm^{-1} for PS II antenna chls).

Another interesting aspect of antenna chl heterogeneity in CP29 is the pronounced overlapping vibrational structure associated with the A2-CHL612 chl but absent in the A3-CHL613 and B3-CHL614 chls. This structure has not been detected either in solvated chls or in calculations of the vibrational band shape of PSI chls from line narrowing spectroscopy (*48*). Based on chl band shape calculations, the OS was suggested to be due to unusually strong coupling to low-frequency phonons (*19*). On the

other hand, it has been suggested recently by Mozzo et al. (*21*) that this may be an high-energy excitonic partner of the A2-CHL612 chl on the basis of a low-temperature absorption measurement and CD measurements. We, however, are in disagreement with this suggestion for three reasons: (i) First is the observation, in the present paper, of the OS absorption/fluorescence mirror symmetry image of the OS in the same frequency range with respect to the mirror symmetry axis, both energetically below (fluorescence) and above (absorption). This evidence would seem to be definitive and indicates quite strong coupling to vibrational frequencies in the 300−600 cm^{-1} range. Of course, for a high-energy excitonic band the mirror symmetry will be absent (*49*). (ii) In the case of the OS representing the high-energy component of a dimer-type interaction with the A2-CHL612 chl, it is expected that the dipole strength of the two chls becomes redistributed over the excitonic state according to their dipole transition vector mutual space position. Thus mutation of the A2-CHL612 chl would lead to a breaking of the excitonic state, with the nonmutated chl undergoing a change in dipole strength. This should be discernible in the wt *minus* mutant absorption spectrum except for the case in which the transition dipoles are orientated close to 90° with respect to each other, and the subsequent dipole strength redistribution over the two excitonic states is approximately equal. While there is clearly no information available for the mutual dipole orientations in CP29, for LHCII these may be determined from the crystallographic structure of Liu et al. (*23*) and indicate that a quite strong interaction occurs between the chls A2-CHL612 and B2-CHL611. In this case our calculations (unpublished data) suggest that the dipole strength distribution factor is about 1.8/0.2 for the low-energy/high-energy bands (data not presented). This would lead to an increase in the dipole strength of the high-energy excitonic partner in the mutant complex (now a monomer) and thus to a negative structure in the difference spectrum. This negative structure is not evident. (iii) Concerning the CD measurements of Mozzo et al. (*21*), they report a small (few millidegree) difference in the positive 665 nm lobe, near the absorption OS, in the A2-CHL612 mutant complex. This was also interpreted in terms of an excitonic interaction with the A2-CHL612 chl. After a careful analysis of the CD signal errors we are unable to agree with these data (Figure 8) as any change of this small magnitude is within our errors distribution. Mozzo at al. (*21*) did not present an error analysis.

An unexpected aspect of the CP29 wt *minus* mutant difference absorption spectra is the presence in both of the cases of the A3-CHL613 and B3-CHL614 chls of pronounced secondary difference spectra structures in the chl *b* wavelength region (640 and 653 nm). Two possible explanations readily present themselves. One is that the B3-CHL614 chl *a*, absorbing near 680 nm, interacts excitonically with the chl *b* molecules. This possibility is ruled out by two considerations. First in the assumption that excitonic interactions exist in CP29 between the A3-CHL613 and B3-CHL614 chl *a* and chl *b*; as mentioned above, it is expected that the dipole strength of these chls becomes redistributed over the excitonic state. Thus, loss of the B3-CHL614 and A3-CHL613 chls by mutation would lead to a breaking of the excitonic state, with the remaining chl undergoing a change in dipole strength. This should be discernible in the wt *minus* mutant absorption difference spectrum, apart from the very peculiar case of no dipole redistribution, as a positive increase in absorption intensity and therefore as a negative difference spectra structure. Instead, the chl *b* difference spectra structures are all positive, which argues against the chl *a*−chl *b* excitonic hypothesis. Second, the CD spectrum of the CP29b3 mutant is indistinguishable from the wt spectrum, and the CP29a3 mutant spectrum shows no significant change in the chl *b* region at 640 nm. Moreover, in LHCII no relevant interactions between the B3-CHL614 or A3-CHL613 and chl *b* have been proposed (*45*). We therefore exclude the excitonic interaction hypothesis for these two chlorophylls.

The second possibility, which has gained considerable support in the literature for a number of chl binding sites in both CP29 and LHCII, is that of "mixed sites"; i.e., during the reconstitution these sites may bind either chl *a* or chl *b* (*3*, *18*, *28*). This interpretation is however open to criticism. First, the atomic resolution crystallographic structure of a number of LHCII trimers (*23*) shows no evidence for mixed sites. In the ten LHCII monomers examined by these authors not even a single mixed site was detected, though it has been suggested that this may be due to the different chl binding conditions *in vivo* with respect to the *in vitro* reconstitution (*50*). Second, it has recently been shown by a detailed analysis of the Liu et al. (*23*) crystallographic structure of LHCII (*19*) that the protein binding sites of both chls *a* and *b* bring about molecular macrocycle distortions which give rise to energy displacements of the electronic transitions. In particular, of the six lowest out-of-plane deformation modes characteristic of the chlorin macrocycle, four have the same symmetry of the HOMO, LUMO and HOMO−1, LUMO+1 molecular orbitals whose energy gaps $\Delta E_{H\rightarrow L}$ and $\Delta E_{H-1\rightarrow L+1}$ are directly involved in determining the electronic transition energy, according to the Gouterman approach (*51*). With respect to the unperturbed situation, when the chl molecule is free from externally imposed deformation, these two unperturbed energy gaps, ΔE^0, become modified by the binding site imposed macrocycle deformation

$$\Delta E_{H\rightarrow L} = \Delta E^0{}_{H\rightarrow L} + \Delta\delta E_{H\rightarrow L}$$

$$\Delta E_{H-1\rightarrow L+1} = \Delta E^0{}_{H-1\rightarrow L+1} + \Delta\delta E_{H-1\rightarrow L+1}$$

with the addition of an energy contribution to the total energy gaps that depends on purely geometrical factors. In the case of LHCII, macrocycle deformations lead to an estimated red shift of the electronic transitions up to 17 nm for chl *a* and up to 11 nm for chl *b*. For CP29, using the LHCII monomer as a model, the previously discussed mutational analysis suggests that both chls B3-CHL614 and A3-CHL613 contribute to the complex absorption spectrum in the extreme red region. We can then hypothesize that both the A3-CHL613 and B3-CHL614 CP29 protein binding sites perturb the chlorin rings in a way that leads to large red shifts of the electronic transitions. In other words, if the A3-CHL613 and B3-CHL614 sites are mixed sites, a maximal red shift should be observed for both chl *a* and chl *b* when present in these sites. Experimental evidence, in qualitative support of this, comes from the earlier study by Giuffra et al. (*28*) in which additional chl *b* was shown to bind to the CP29 wt complex by performing the reconstitution at high relative concentrations of chl *b*. It was shown that when chl *b* substituted chl *a* at its binding site, the chl *b* underwent red shifting. This is clearly not the present case, as in the A3-CHL613 and B3-CHL614 chl difference spectra (Figures 5B and 6B) both the 640 and 653 nm chl *b* absorption maxima are unchanged with respect to those of the two chls *b* in the wt complex (Figures 4−6). In addition, we point out that if the single molecular species (chl *b*) were to bind to the same site (A3-CHL613 or B3-CHL614 binding site), it is difficult

to see how this would generate two absorption spectral forms absorbing at 640 and 653 nm. Thus we exclude that the A3-CHL613 and B3-CHL614 chl binding sites are so-called "mixed sites".

An explanation concerning the effect of the mutations of the chl *a* binding sites B3-CHL614 and A3-CHL613 is therefore not readily forthcoming in these terms. Thus we, somewhat unwillingly, are forced to suggest that these two mutations, while not leading to significant structural changes in the CP29 complex, as indicated by the respective CD and absorption spectra, seem to lower the binding constant(s) for chl *b* to a small extent. In this eventuality a small fraction of reconstituted complexes may not bind either one or both of the two chl *b* molecules, in the case of the B3-CHL614 and A3-CHL613 mutations. This suggestion gains experimental support from the following observations. The mean chl *a*/*b* ratio of the CP29a2 mutant complex was determined as 2.5 (Materials and Methods section), consistent with the loss of one chl *a*, when compared with the wt complex mean chl *a*/*b* = 3.0). The A2-CHL612 difference spectrum shows changes *only* in the chl *a* spectral region. On the other hand, as discussed above, the B3-CHL614 mutation shows quite a large decrease in the difference spectra structure in the chl *b* region (640 and 653 nm) and a high chl *a*/*b* ratio of 3.5. This ratio is readily explained by the loss of, on average, one chl *a* and 0.5 chl *b* per complex, as we have already excluded the possibility of "mixed" chl *a*/*b* binding sites. An apparently similar situation is found for the A3-CHL613 mutation, which displays a small difference spectrum decrease in the chl *b* region at 640 nm and has a mean chl *a*/*b* ratio of 2.7.

In the present paper we argue against the idea of the A3-CHL613 and B3-CHL614 binding sites being mixed with respect to their chl *a* and *b* binding capacity. This interpretation is based on chl binding to the CP29 complex under conditions in which the wt complex has the correct, native complex, binding ratio of close to 3.0. The idea of mixed sites originally was largely based on experiments in which the relative chl *b* concentration during reconstitution was high (e.g., ref *28*). Under these conditions additional chl *b* binds to CP29wt in substitution for chl *a*. Our point is therefore that while chl *b* may, in fact, bind to chl *a* sites when the reconstitution conditions are "forced", the binding constants of the A3 and B3 sites normally ensure selection for chl *a*.

REFERENCES

1. Jennings, R. C., Zucchelli, G., and Garlaschi, F. M. (1990) Excitation energy transfer from the chl spectral forms to photosystem II reaction centres: a fluorescence induction study. *Biochim. Biophys. Acta 1016*, 259–265.
2. Zucchelli, G., Dainese, P., Jennings, R. C., Breton, J., Garlaschi, F. M., and Bassi, R. (1994) Gaussian decomposition of absorption and linear dichroism spectra of outer antenna complexes of photosystem II. *Biochemistry 33*, 8982–8990.
3. Salverda, J. M., Vengris, M., Krueger, B. P., Scholes, G. D., Czamoleski, A. R., Novoderezhkin, V., van Amerongen, H., and van Grondelle, R. (2003) Energy transfer in light-harvesting complexes LHCII and CP29 of spinach studied with three pulse echo peak shift and transient grating. *Biophys. J. 84*, 450–465.
4. Jennings, R. C., Bassi, R., and Zucchelli, G. (1996) Antenna structure and energy transfer in higher plants photosystems. *Top. Curr. Chem. 177*, 147–181.
5. Gradinaru, C. C., Ozdemir, S., Gulen, D., van Stokkum, I. H. M., van Grondelle, R., and van Amerongen, H. (1998) The flow of excitation energy in LHCII monomers: Implications for the structural model of the major plant antenna. *Biophys. J. 75*, 3064–3077.
6. Jennings, R. C., Elli, G., Garlaschi, F. M., Santabarbara, S., and Zucchelli, G. (2000) Selective quenching of the fluorescence of core chl-protein complexes by photochemistry indicates that photosystem II is partly diffusion limited. *Photosynth. Res. 66*, 225–233.
7. Barzda, V., Gulbinas, V., Kananavicius, R., Cervinskas, V., van Amerongen, H., van Grondelle, R., and Valkunas, L. (2001) Singlet-singlet annihilation kinetics in aggregates and trimers of LHCII. *Biophys. J. 80*, 2409–2421.
8. Vasil'ev, S., Orth, P., Zouni, A., Owens, T. G., and Bruce, D. (2001) Excited-state dynamics in photosystem II: Insights from the x-ray crystal structure. *Proc. Natl. Acad. Sci. U.S.A. 98*, 8602–8607.
9. Miloslavina, Y., Szczepaniak, M., Muller, M. G., Sander, J., Nowaczyk, M., Rogner, M., and Holzwarth, A. R. (2006) Charge separation kinetics in intact photosystem II core particles is trap-limited. A picosecond fluorescence study. *Biochemistry 45*, 2436–2442.
10. Tumino, G., Casazza, A. P., Engelmann, E., Garlaschi, F. M., Zucchelli, G., and Jennings, R. C. (2008) Fluorescence lifetime spectrum of the plant photosystem II core complex: Photochemistry does not induce specific reaction center quenching. *Biochemistry 47*, 10449–10457.
11. Förster, T. (1959) Transfer mechanisms of electronic excitation. *Discuss. Faraday Soc. 27*, 7–16.
12. Berthold, D. A., Babcock, G. T., and Yocum, C. F. (1981) A highly resolved oxygen evolving photosystem II preparation from spinach thylacoid membranes. EPR and electron transport properties. *FEBS Lett. 134*, 231–234.
13. Nield, J., Orlova, E. V., Morris, E. P., Gowen, B., van Heel, M., and Barber, J. (2000) 3D map of the plant photosystem II supercomplex obtained by cryoelectron microscopy and single particle analysis. *Struct. Biol. 7*, 44–47.
14. Zouni, A., Witt, H. T., Kern, J., Fromme, P., Krauss, N., Saenger, W., and Orth, P. (2001) Crystal structure of photosystem II from *Synechococcus elongatus* at 3.8 angstrom resolution. *Nature 409*, 739–743.
15. Jennings, R. C., Bassi, R., Garlaschi, F. M., Dainese, P., and Zucchelli, G. (1993) Distribution of the chl spectral forms in the chl-protein complexes of photosystem II antenna. *Biochemistry 32*, 3203–3210.
16. Zucchelli, G., Cremonesi, O., Garlaschi, F. M., and Jennings, R. C. (1998) Förster overlap integral for chl *a* in a protein matrix, in Photosyntesis: Mechanisms and Effects (Garab, G., Ed.) pp 449−452, Kluwer Academic Publishers, Dordrecht/Boston/Lancaster.
17. Gillie, J. K., Small, G. J., and Golbeck, J. H. (1989) Nonphotochemical hole burning of the native antenna complex of photosystem I (PS I-200). *J. Phys. Chem. 93*, 1620–1627.
18. Bassi, R., Croce, R., Cugini, D., and Sandona, D. (1999) Mutational analysis of a higher plant antenna protein provides identification of chromophores bound into multiple sites. *Proc. Natl. Acad. Sci. U.S.A. 96*, 10056–10061.
19. Zucchelli, G., Jennings, R. C., Garlaschi, F. M., Cinque, G., Bassi, R., and Cremonesi, O. (2002) The calculated in vitro and in vivo chl *a* absorption bandshape. *Biophys. J. 82*, 378–390.
20. Pascal, A., Peterman, E., Gradinaru, C., van Amerongen, H., van Grondelle, R., and Robert, B. (2000) Structure and interactions of the chl *a* molecules in the higher plant Lhcb4 antenna protein. *J. Phys. Chem. B 104*, 9317–9321.
21. Mozzo, M., Passarini, F., Bassi, R., van Amerongen, H., and Croce, R. (2008) Photoprotection in higher plants: The putative quenching site is conserved in all outer light-harvesting complexes of photosystem II. *Biochim. Biophys. Acta 1777*, 1263–1267.
22. Kühlbrandt, W., Wang, D. N, and Fujiyoshi, Y. (1994) Atomic model of plant light-harvesting complex by electron crystallography. *Nature 367*, 614–621.
23. Liu, Z. F., Yan, H. C., Wang, K. B., Kuang, T. Y., Zhang, J. P., Gui, L. L., An, X. M., and Chang, W. R. (2004) Crystal structure of spinach major light-harvesting complex at 2.72 angstrom resolution. *Nature 428*, 287–292.
24. Paulsen, H., Rumler, U., and Rudiger, W. (1990) Reconstitution of pigment-containing complexes from light harvesting chl *a*/*b* binding protein overexpressed in *Escherichia coli*. *Planta 181*, 204–211.
25. Giuffra, E., Cugini, D., Croce, R., and Bassi, R. (1996) Reconstitution and pigment-binding properties of recombinant CP29. *Eur. J. Biochem. 238*, 112–120.
26. Sandona, D., Croce, R., Pagano, A., Crimi, M., and Bassi, R. (1998) Higher plants light harvesting proteins structure and function as revealed by mutation analysis of either protein or chromophore moieties. *Biochim. Biophys. Acta 1365*, 207–214.
27. Bassi, R., Hoyer-Hansen, G., Barbato, R., Giacometti, G. M., and Simpson, D, J. (1987) Chl-proteins of the photosystem II antenna system. *J. Biol. Chem. 262*, 13333–13341.
28. Giuffra, E., Zucchelli, G., Sandona, D., Croce, R., Cugini, D., Garlaschi, F. M., Bassi, R., and Jennings, R. C. (1997) Analysis of

some optical properties of a native and reconstituted photosystem II antenna complex, CP29: Pigment binding sites can be occupied by chl *a* or chl *b* and determine spectral forms. *Biochemistry 36*, 12984–12993.
29. Davies, B. H. (1976) Carotenoids, in Chemistry and Biochemistry of Plant Pigments (Goodwin, T. W., Ed.) pp 38−165, Academic Press, New York.
30. Porra, R. J., Thompson, W. A., and Kriedermann, P. E. (1989) Determination of accurate extinction coefficients and simultaneous equations for assaying chls *a* and *b* extracted with four different solvents: Verification of the concentration of chl standards by atomic absorption spectroscopy. *Biochim. Biophys. Acta 975*, 384–394.
31. Lichtenthaler, H. K. (1987) Chls and carotenoids: Pigments of photosynthetic biomembranes. *Methods Enzymol. 148*, 351–382.
32. Cattaneo, R., Zucchelli, G., Garlaschi, F. M., Finzi, L., and Jennings, R. C. (1995) A thermal broadening analysis of absorption spectra of the d1/d2/cytochrome *b*-559 complex in terms of Gaussian decomposition sub-bands. *Biochemistry 34*, 15267–15275.
33. Hayes, J. M., Gillie, J. K., Tang, D., and Small, G. J. (1988) Theory for spectral hole burning of the primary electron donor state of photosynthetic reaction centers. *Biochim. Biophys. Acta 932*, 287–305.
34. Stepanov, B. I. (1957) A universal relation between the absorption and luminescence spectra of complex molecules. *Dokl. Akad. Nauk SSSR 112*, 839–843.
35. Knox, R. S., and Marshall, L. F. (2000) The Kennard-Stepanov relation for time-resolved fluorescence. *J. Luminesc. 85*, 209–215.
36. Pascal, A., Gradinaru, C., Wacker, U., Peterman, E., Calkoen, F., Irrgang, K. D., Horton, P., Renger, G., van Grondelle, R., Robert, B., and van Amerongen, H. (1999) Spectroscopic characterization of the spinach Lhcb4 protein (CP29), a minor light-harvesting complex of photosystem II. *Eur. J. Biochem. 262*, 817–823.
37. Houssier, C., and Sauer, K. (1970) Circular dichroism and magnetic circular dichroism of the chl and protochl pigments. *J. Am. Chem. Soc. 92*, 779–791.
38. Kropacheva, T. N., Germano, M., Zucchelli, G., Jennings, R. C., and van Gorkom, H. J. (2005) Circular dichroism of the peripheral chls in photosystem II reaction centers revealed by electrochemical oxidation. *Biochim. Biophys. Acta 1709*, 119–126.
39. Büchel, C., and Garab, G. (1997) Organization of the pigment molecules in the chlorophyll *a*/*c* light-harvesting complex of *Pleurochloris meiringensis* (Xanthophyceae). Characterization with circular dichroism and absorbance spectroscopy. *J. Photochem. Photobiol., B 37*, 118–124.
40. Garab, G., and van Amerongen, H. (2009) Linear dichroism and circular dichroism in photosynthesis research. *Photosynth. Res. 101* (2−3), 135–146.
41. Zucchelli, G., Brogioli, D., Casazza, A. P., Garlaschi, F. M., and Jennings, R. C. (2007) Chl ring deformation modulates Q_y electronic energy in chl-protein complexes and generates spectral forms. *Biophys. J. 93*, 2240–2254.
42. Gillie, J. K., Hayes, J. M., Small, G. J., and Golbeck, J. H. (1987) Hole burning spectroscopy of a core antenna complex. *J. Phys. Chem. 91*, 5524–5527.
43. Cattaneo, R., Finzi, L., Zucchelli, G., Garlaschi, F. M., and Jennings, R. C. (1995) Thermal broadening of Gaussian subbands of the reaction centre complex of photosystem II, in Photosynthesis: from Light to Biosphere (Mathis, P., Ed.) pp 187−190, Kluwer Academic Publishers, Dordrecht/Boston/London.
44. Nelson, N., and Yocum, C. F. (2006) Structure and function of photosysthem I and II. *Annu. Rev. Plant Biol. 57*, 521–565.
45. Frahmcke, J. S., and Walla, P. J. (2006) Coulombic couplings between pigments in the major light-harvesting complex LHC II calculated by the transition density cube method. *Chem. Phys. Lett. 430*, 397–403.
46. Pieper, J., Irrgang, K. D., Ratsep, M., Voigt, J., Renger, G., and Small, G, J. (2000) Assignment of the lowest Q(y)-state and spectral dynamics of the CP29 chl *a*/*b* antenna complex of green plants: A hole-burning study. *Photochem. Photobiol. 71*, 574–581.
47. Ratsep, M., Pieper, J., Irrgang, K. D., and Freiberg, A. (2008) Excitation wavelength-dependent electron-phonon and electron-vibrational coupling in the CP29 antenna complex of green plants. *J. Phys. Chem. B 112*, 110–118.
48. Jia, Y., Jean, J. M., Werst, M. M., Chan, C. K., and Fleming, G. R. (1992) Simulations of the temperature dependence of energy transfer in the PSI core antenna. *Biophys. J. 63*, 259–273.
49. Lakowicz, J. R. (1983) Principles of Fluorescence Spectroscopy, Plenum Press, New York.
50. Horn, R., Grundmann, G., and Paulsen, H. (2007) Consecutive binding of chls *a* and *b* during the assembly in vitro of light-harvesting chl-*a*/*b* protein (LHCIIb). *J. Mol. Biol. 366*, 1045–1054.
51. Gouterman, M. (1961) Spectra of phorphyrins. *J. Mol. Spectrosc. 6*, 138–163.